A&A 628, A126 (2019)
https://doi.org/10.1051/0004-6361/201935952

Astronomy & Astrophysics

Revisiting the 16 Cygni planet host at unprecedented precision and exploring automated tools for precise abundances

M. Tucci Maia[1,2], J. Meléndez[3], D. Lorenzo-Oliveira[3], L. Spina[3], and P. Jofré[1]

[1] Núcleo de Astronomía, Facultad de Ingeniería, Universidad Diego Portales, Av. Ejército 441, Santiago, Chile
e-mail: marcelo.tucci@mail.udp.cl
[2] Laboratorio Nacional de Astrofísica, Rua dos Estados Unidos 154, Itajubá, 37504-364 Minas Gerais, MG, Brazil
[3] Departamento de Astronomia do IAG/USP, Universidade de São Paulo, SP, Brazil

Received 24 May 2019 / Accepted 6 June 2019

ABSTRACT

The binary system 16 Cygni is key in studies of the planet-star chemical composition connection, as only one of the stars is known to host a planet. This allows us to better assess the possible influence of planet interactions on the chemical composition of stars that are born from the same cloud and thus should have a similar abundance pattern. In our previous work, we found clear abundance differences for elements with $Z \leq 30$ between both components of this system and a trend of these abundances as a function of the condensation temperature (T_c), which suggests a spectral chemical signature related to planet formation. In this work we show that our previous findings are still consistent even if we include more species, such as the volatile N and neutron capture elements ($Z > 30$). We report a slope with T_c of $1.56 \pm 0.24 \times 10^{-5}$ dex K^{-1}, that is good agreement with our previous work. We also performed some tests using ARES and iSpec to measure automatically the equivalent width and found T_c slopes in reasonable agreement with our results as well. In addition, we determined abundances for Li and Be by spectral synthesis, finding that 16 Cyg A is richer not only in Li but also in Be, when compared to its companion. This may be evidence of planet engulfment, indicating that the T_c trend found in this binary system may be a chemical signature of planet accretion in the A component, rather than an imprint of the giant planet rocky core formation on 16 Cyg B.

Key words. Sun: abundances – stars: abundances – stars: solar-type – planet–star interactions

1. Introduction

The most accepted hypothesis of star formation is nebular collapse, when stars are formed from gravitationally unstable molecular clouds. Therefore, it is expected that stars that are born from the same interstellar material cloud should have the same abundance pattern during the main sequence, with the exception of the light elements Li and Be, which can be destroyed in regions deeper than the convective zone in solar type stars. Thereby, differences in the chemical content of stars born from the same natal cloud may suggest that extra processes that are not necessary connected to stellar evolution may have influenced the photospheric chemical composition of this cloud. In particular, planet formation or planet engulfment may imprint important chemical signatures in the host star.

Such phenomenon is expected to leave subtle signs on the stellar abundance pattern, on the order of 0.01 dex (Chambers 2010), that can only be detected with a high-precision analysis. This can only be achieved with the differential method (Nissen & Gustafsson 2018), requiring a comparison between the target star with a similar star of known parameters, which serves as the standard for the abundance calculations. So, the sample should be restricted to objects that are very similar among themselves, such as in the case of solar twins[1].

Following this premise, Meléndez et al. (2009) analyzed the abundances of 11 solar twins, achieving a high-precision abundance determination with uncertainties of ∼0.01 dex. These authors found not only a depletion of refractory elements, when compared to the average of the sample, but also a trend with condensation temperature (T_c). The authors suggested that the correlation of the refractory elements abundances with condensation temperature is probably due to rocky planet formation. This hypothesis has been corroborated by Chambers (2010), who showed that the depleted material in the convective zone of the Sun is comparable to the mass of terrestrial planets of our solar system (see also Galarza et al. 2016).

However, other hypotheses have been proposed to explain the abundance trend, such as the stellar environment in which the star was formed (Önehag et al. 2014), although according to recent theoretical estimates by Gustafsson (2018) this mechanism is hardly significant; dust segregation in the protostellar disk (Gaidos 2015); the influence of the stellar age (Adibekyan et al. 2014); and the planet engulfment scenario (Spina et al. 2015).

In this context, twin stars in binary systems are extremely important because the effects connected to the stellar environment of its formation and to the Galaxy chemical evolution would be canceled out in a comparative analysis between both components. Thus, investigating wide binaries can bring more light into the subject of planets interactions (or other astrophysical events) influencing photospheric abundance of their host stars.

[1] More recently, solar twins have been defined as stars with effective temperature within 100 K, log g, and [Fe/H] within 0.1 dex from the Sun (Ramírez et al. 2014).

Some authors have already reported a T_c trend on binary stars. Teske et al. (2016a) found an abundance trend on the WASP94 system, where both stars are planet hosts. The planet-hosting binaries XO-2N/XO-2S (Ramírez et al. 2015; Biazzo et al. 2015; Teske et al. 2015), HD 133131A/B (Teske et al. 2016b), and HAT-P-4 (Saffe et al. 2017), have also shown chemical anomalies most likely due to planets; the binary $\zeta^{1,2}$ Ret, where one of the stars hosts a debris disk, also shows a trend with condensation temperature (Saffe et al. 2016; Adibekyan et al. 2016). Albeit no differences have been found in HAT-P-1 (Liu et al. 2014), HD 80606/HD 80607 (Saffe et al. 2015; Mack et al. 2016), and HD 20782/HD 20781 (Mack et al. 2014) and HD 106515 (Saffe et al. 2019), the evidence is inconclusive in the latter three as a consequence of high abundance errors. Indeed, a more precise abundance analysis of the pair HD 80606/HD 80607 by Liu et al. (2018) shows small but detectable abundance differences between the binary components. HD 240429/HD 240430 is a binary system of twin stars with large abundance differences (Oh et al. 2018), for which no planets are known yet. Furthermore, it was found that Kepler-10, a star hosting a rocky planet, is deficient in refractory elements when compared to stars with similar stellar parameters and from the same stellar population (Liu et al. 2016a).

For 16 Cygni, a binary pair of solar twins, where the B component hosts a giant planet (Cochran et al. 1997), Laws & Gonzalez (2001) clearly detected that 16 Cyg A is more metal rich Δ[Fe/H] = +0.025 ± 0.009 dex than its companion. Later, Ramírez et al. (2011) expanded the analysis to 23 chemical elements, showing abundance differences in all of these by about +0.04 dex and finding a T_C trend similar to Meléndez et al. (2009), when the binary stars are compared to the Sun. This was confirmed in our previous work (Tucci Maia et al. 2014), where we showed that 16 Cyg A is 0.047 ± 0.005 dex metal richer than B and also finding a T_c slope of $+1.99 \pm 0.79 \times 10^{-5}$ dex K^{-1} for the refractory elements, as reported in Ramírez et al. (2011). This result was then associated with the rocky core formation of the gas giant 16 Cyg Bb. Recently, Nissen et al. (2017) also found a Δ[Fe/H](A–B) = +0.031 ± 0.010 dex and a T_c slope of $+0.98 \pm 0.35 \times 10^{-5}$ dex K^{-1}.

In contrast, there are studies that challenge the metallicity difference and the T_c trend between the two components of this system. Schuler et al. (2011) found a T_c trend for both stars relative to the Sun but, however, did not find any significant abundance differences between the pair, which agrees with Deliyannis et al. (2000) and Takeda et al. (2011). Also, Adibekyan et al. (2016), analyzing the case of $\zeta^{1,2}$ Ret, argues that the T_c slope trend could be from nonphysical factors and related to the quality of spectra employed, which is expected as high-precision abundances can only be obtained in spectra of adequate quality.

In this context, the initial motivation for this work is to assess if, by revisiting this binary system now with better data with higher resolving power, higher S/N, and broader spectral coverage, our previous results (obtained with lower resolving power) would still be consistent. In addition we include the analysis of elements that were not available before to provide improvements in the precision of the abundance determination. We also challenge our results by employing automated tools to derive stellar parameters and T_c while using the same methodology in all of the cases.

On the following sections, we present the differential abundances of 34 elements and the abundances of Li and Be, through spectral synthesis, which may present possible evidence of planetary engulfment on 16 Cyg A.

2. Data and analysis

2.1. Observations and data reduction

The observations of 16 Cyg A and B were carried out in June 2015 with the High Dispersion Spectrograph (HDS; Noguchi et al. 2002) on the 8.2 m Subaru Telescope of the National Astronomical Observatory of Japan (NAOJ), located at the Mauna Kea summit. Besides the 16 Cyg Binary system, we also observed the asteroid Vesta, which was used as an initial reference for our differential analysis.

For the optical, we obtained a S/N of ∼750 at 600 nm and ∼1000 at 670 nm (Li region) on the highest resolution possible ($R \sim 160\,000$) using the 0.2″ slit. The UV observations with HDS were made using the 0.4″ slit, which provides a $R = 90\,000$ that results in an $S/N \sim 350$ per pixel at 340 nm, corresponding to the NH region, and $S/N \sim 200$ at 310 nm (Be region). This gave us the opportunity to analyze volatile elements such as nitrogen and neutron-capture elements in the UV with $S/N > 300$.

The stars from the binary system and the Sun (Vesta) were both observed using the same instrumental setup to minimize errors in a differential analysis, which requires a comparisons between the spectra of all sample stars for the continuum placement and a comparison of the line profiles to achieve consistent equivalent width (EW) measurements.

The extraction of the orders and wavelength calibration were performed immediately after the observations by Subaru staff with routines available at the observatory. The continuum normalization and Doppler correction were performed using standard routines with the Image Reduction and Analysis Facility (IRAF).

2.2. Stellar parameters

Our method to determine stellar parameters and elemental abundances follows the approach described in previous papers (e.g., Ramírez et al. 2011, 2014; Meléndez et al. 2009, 2012; Tucci Maia et al. 2016; Spina et al. 2016), in which differential excitation and ionization equilibrium for Fe I and Fe II lines are imposed (Fig. 1). Since the 16 Cygni system is a pair of solar twins, they have similar physical characteristics to the Sun, and thus we initially used the Sun as a reference for our analysis.

The abundance determination was performed using the line-by-line differential method, employing the EW manually measured by fitting Gaussian profiles with the IRAF *splot* task and deblending when necessary. Very special care was taken for the continuum placement during the measurements, always comparing and overplotting the spectral lines region for the sample, and focusing on a consistent determination.

With the measured EW, we first determined the Fe I and Fe II abundances to differentially obtain the stellar parameters. For this we employed the 2014 version of the LTE code MOOG (Sneden 1973) with the MARCS grid of 1D-LTE model atmospheres (Gustafsson et al. 2008). It is important to highlight that the choice of a particular atmospheric model has a minor impact on the determination of stellar parameters and chemical abundances in a strictly differential analysis, as long the stars that are being studied are similar to the star of reference (e.g., Tucci Maia et al. 2016).

To make the analysis more efficient, we employed the Python q^2 code[2] (Ramírez et al. 2014), which operates in a semiautomatic mode, by calling MOOG routines to determine the elemental abundances and we performed a line-by-line differential

[2] https://github.com/astroChasqui/q2

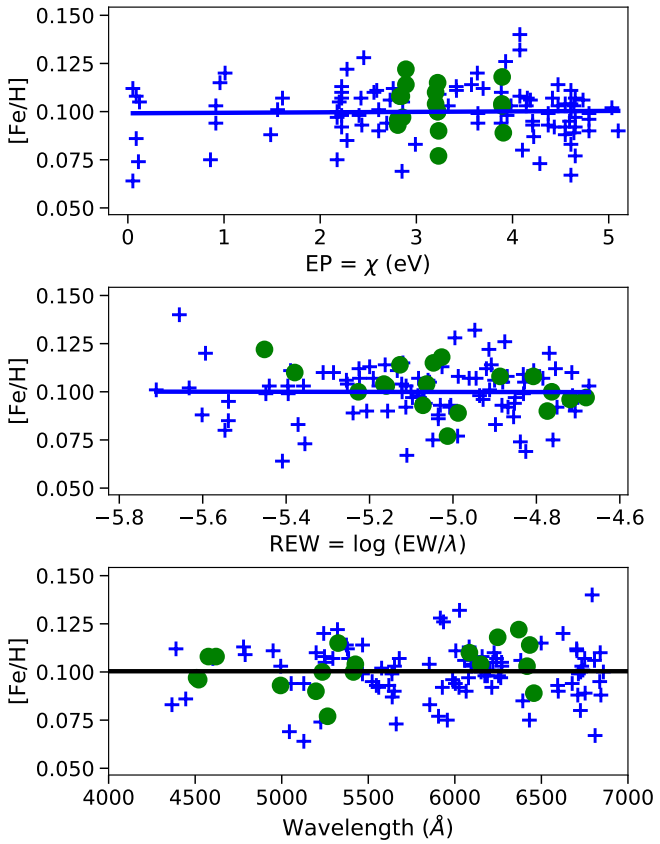

Fig. 1. Excitation and ionization equilibrium of Fe abundances (manually measured) using the Sun as the standard star for 16 Cyg A. Crosses represent Fe I and filled circles Fe II.

analysis using these results. This code also performs corrections of hyperfine structure (HFS) and the determination of uncertainties. In this work, we take into account the HFS for V, Mn, Co, Cu, Y, Ag, La, and Pr using the line list from Meléndez et al. (2012). The errors are computed considering both observational (due to uncertainties in the measurements, represented by the standard error) and systematic uncertainties (from the stellar parameters and their interdependences), as described in Ramírez et al. (2015). Observational and systematic errors are added in quadrature.

Table 1 shows the stellar parameters obtained for 16 Cyg A and B using the Sun ($T_{\rm eff}$ = 5777 K, log g = 4.44 dex, [Fe/H] = 0.0 dex) as reference. We note that these results are practically the same within the errors as those found in Tucci Maia et al. (2014), which are $T_{\rm eff} = 5830 \pm 7$ K, log $g = 4.30 \pm 0.02$, and [Fe/H] = 0.101 ± 0.008 dex for 16 Cyg A, and $T_{\rm eff} = 5751 \pm 7$ K, log $g = 4.35 \pm 0.02$, and [Fe/H] = 0.054 ± 0.008 dex for 16 Cyg B. The final difference in metallicity between the components of this binary system is remarkably similar to that reported in Tucci Maia et al. (2014), that is Δ[Fe/H] = 0.047 ± 0.005 dex, while we find in this work Δ[Fe/H] = 0.040 ± 0.006 dex. This confirms with a significance of $\sim 7\sigma$ that 16 Cyg A is indeed more metal rich when compared to 16 Cyg B, in agreement with Ramírez et al. (2011), the earlier work by Laws & Gonzalez (2001), and the recent work by Nissen et al. (2017).

2.3. Trigonometric surface gravity

New parallaxes for the binary stars of 16 Cygni have been measured by the *Gaia* mission DR 2 (Gaia Collaboration 2018). The new values are 47.2771 ± 0.0327 mas and 47.2754 ± 0.0245 mas for 16 Cyg A and B, respectively. Adopting the magnitudes from the General Catalogue of Photometric Data (Mermilliod et al. 1997) with $V(\rm A) = 5.959 \pm 0.009$ and $V(\rm B) = 6.228 \pm 0.019$, we determined the absolute magnitudes $M_{\rm A} = 4.332 \pm 0.012$ and $M_{\rm B} = 4.599 \pm 0.026$. Using this information with the values of the $T_{\rm eff}$, metallicity and mass, we estimated the trigonometric surface gravity for the pair of stars. For 16 Cyg A we found log $g(A_{\rm T}) = 4.293 \pm 0.005$ dex and for 16 Cyg A log $g(B_{\rm T}) = 4.364 \pm 0.006$. We note that, while the surface gravity for 16 Cyg B has a good agreement with that found through the ionization equilibrium of Fe lines (Table 1), for 16 Cyg A the trigonometric value is ~0.02 dex lower, albeit they agree within 1.5σ. In comparison with the results of Ramírez et al. (2011), both the trigonometric and Fe-lines-based surface gravity are in agreement for the A component, while our surface gravities for B are somewhat higher in both cases.

Table 1. Stellar parameters for the 16 Cygni binary system using EW measured manually.

	16 Cyg A	16 Cyg B
$T_{\rm eff}$ (K)	5832 ± 5	5763 ± 5
log g (dex)	4.310 ± 0.014	4.360 ± 0.014
log g (dex)$_{\rm trigonometric}$	4.293 ± 0.005	4.364 ± 0.006
[Fe/H] (dex)	0.103 ± 0.004	0.063 ± 0.004
$v_{\rm t}$ (km s^{-1})	1.11 ± 0.01	1.03 ± 0.01
Luminosity$(L_\odot)_{\log g}$	1.46 ± 0.05	1.19 ± 0.04
Luminosity$(L_\odot)_{\rm parallax}$	1.55 ± 0.02	1.23 ± 0.02
Mass $(M_\odot)_{\log g}$	1.06 ± 0.02	1.01 ± 0.01
Mass $(M_\odot)_{\rm parallax}$	1.06 ± 0.01	1.01 ± 0.01
Radius $(R_\odot)_{\log g}$	1.19 ± 0.02	1.09 ± 0.02
Radius $(R_\odot)_{\rm parallax}$	1.18 ± 0.02	1.12 ± 0.01
Age (Gyr)$_{\log g}$	6.0 ± 0.3	6.8 ± 0.4
Age (Gyr)$_{\rm parallax}$	6.4 ± 0.2	7.1 ± 0.2
Age (Gyr)$_{\rm [Y/Mg]}$	6.2 ± 1.0	6.3 ± 1.0
Age (Gyr)$_{\rm [Y/Al]}$	6.6 ± 1.0	6.8 ± 1.0

2.4. Age, mass, and radius

The age and mass of the binary stars were determined using customized Yonsei-Yale isochrones (Yi et al. 2001), as described in Ramírez et al. (2013, 2014). This method provides good relative ages owing to the high precision achieved for the atmospheric parameters. We estimate the ages and masses with probability distribution functions, through the comparison of atmospheric parameters position of the star with the values predicted by the isochrones. Initially, the calculations were based on the [Fe/H], $T_{\rm eff}$, and log g, and later we replaced the gravity by the parallax values and magnitudes to obtain the isochronal ages using the absolute magnitudes. The results are shown in Table 1. Our masses and radii show a very good agreement when compared to the asteroseismology determinations of $M_{\rm A} = 1.08 \pm 0.02\ M_\odot$, $M_{\rm B} = 1.04 \pm 0.02\ M_\odot$, $R_{\rm A} = 1.229 \pm 0.008\ R_\odot$, and $R_{\rm B} = 1.116 \pm 0.006\ R_\odot$, as reported by Metcalfe et al. (2015).

The inferred isochronal ages of A and B based on log g are 6.0 ± 0.3 and 6.7 ± 0.4 Gyr, respectively. This shows that both components of the system have roughly the same age (within error bars). We also estimated the ages of 16 Cyg A and B using the correlation of [Y/Mg] and [Y/Al] as a function of stellar age. The abundance clock [Y/Mg] for solar-type stars was first suggested by da Silva et al. (2012) and the correlation between

Table 2. Activity indexes for 16 Cyg A, B, and the Sun.

Star	$\mathcal{H}$
Sun	0.1909 ± 0.0019
16 Cyg A	0.1871 ± 0.0021
16 Cyg B	0.1889 ± 0.0021
16 Cyg AB	0.1880 ± 0.0010

Notes. The last row is the mean activity level of 16 Cyg AB.

[Y/Mg] or [Y/Al] and stellar age was quantified for solar twins by Nissen (2015), Tucci Maia et al. (2016), and Spina et al. (2016)[3]. The derived [Y/Mg] ages are $A = 6.2$ Gyr and $B = 6.3$ Gyr using the relation of Tucci Maia et al. (2016). Similar ages are found using the Spina et al. (2016) relations $A = 6.0 \pm 1.0$ Gyr and $B = 6.1 \pm 1.0$ Gyr. These results are consistent with the values calculated using the isochronal method, while the [Y/Al] ages (Spina et al. 2016) give $A = 6.6 \pm 1.0$ Gyr and $B = 6.8 \pm 1.0$ Gyr. The values of age, mass, and radius agree with asteroseismic with values around 7 Gyrs (van Saders et al. 2016; Bellinger et al. 2017); 16 Cyg A is slightly more massive and has a bigger radius than its companion.

2.5. Activity

The chromospheric activity is an important constraint on stellar ages (Lorenzo-Oliveira et al. 2018). In order to measure the activity differences between 16 Cyg A and B, we defined an instrumental activity index based on Hα line that is a well-known chromospheric indicator of late-type stars (Pasquini & Pallavicini 1991; Lyra & Porto de Mello 2005; Montes et al. 2001), i.e.

$$\mathcal{H} = \frac{F_{\mathrm{H}\alpha}}{(F_{\mathrm{B}} + F_{\mathrm{V}})}, \quad (1)$$

where $F_{\mathrm{H}\alpha}$ is the flux integrated around the Hα line ($\Delta\lambda = 6562.78 \pm 0.3$ Å). We chose this narrow spectral interval to minimize the effective temperature effects that might be present along the Hα wings[4]. The values F_{B} and F_{V} are the fluxes integrated around 0.3 Å continuum windows, centered at 6500.375 and 6625.550 Å, respectively. In Table 2, we show the estimated $\mathcal{H}$ for 16 Cyg AB and the Sun. The uncertainties were estimated by quadratic error propagation of Eq. (1), assuming Poisson error distribution.

Accordingly to $\mathcal{H}$, none of 16 Cyg components show an unexpected level of chromospheric activity for a typical 6–7 Gyr star (Mamajek & Hillenbrand 2008). Furthermore, 16 Cyg A and B seem to be chromospherically quiet stars ($\mathcal{H} = 0.188 \pm 0.001$) and slightly more inactive than the Sun ($\mathcal{H} = 0.1909 \pm 0.0019$), indicating a chromospheric age older than 4–5 Gyr. This result is in line with Ca II H & K multi-epoch observations of Isaacson & Fischer (2010) who found $\log(R'_{\mathrm{HK}}) \approx -5.05$ dex for this system. This finding is in good agreement with the mean activity level of $\log(R'_{\mathrm{HK}}) = -5.03 \pm 0.1$ dex derived for 49 solar-type stars from the 6–7 Gyr old open cluster NGC 188 (Lorenzo-Oliveira et al. 2016a).

[3] The correlation between [Y/Mg] and age is only valid for solar-metallicity stars (Feltzing et al. 2017).

[4] Small residual photospheric effects are still expected to be affecting our index measurements, however, this residual feature should have negligible impact on our results since we are not interested in absolute activity scale determination for a wide range of effective temperatures.

We inspected the chromospheric signature of other classical indicators along the spectral coverage of our observations such as Ca II H & K (Mamajek & Hillenbrand 2008; Lorenzo-Oliveira et al. 2016a), Hβ (Montes et al. 2001), and Ca II infrared triplet (Lorenzo-Oliveira et al. 2016b). All of these show the same behavior found by Hα lines; 16 Cyg A and B are chromospherically older than the Sun (age > 4–5 Gyr) and the activity differences between the components are negligible. In summary, the different activity indicators reinforce the age results from isochrones and seismology.

3. Abundance analysis

We present high-precision abundances for the light elements C, N, O, Na, Mg, Al, Si, S, K, Ca, Sc, Ti, V, Cr, Mn, Co, Ni, Cu, and Zn; and the heavy elements Sr, Y, Zr, Ba, Ru, Rh, Pd, Ag, La, Ce, Nd, Sm, Eu, Gd, and Dy. The abundances of these elements were differentially determined using initially the Sun as our standard star and then using 16 Cyg B as the reference to obtain the $\Delta[\mathrm{X/H}]_{(A-B)}$. The calculations were performed with the same method as described for the iron lines (see also Tucci Maia et al. 2016).

Taking into account only the elements with $Z \leq 30$, there is a clear chemical trend as a function of the condensation temperature (T_{c}) in the pattern of both stars relative to the Sun (Fig. 2), which agrees with Ramírez et al. (2011), Schuler et al. (2011) and Tucci Maia et al. (2014). In addition to results based on atomic lines, abundances for the volatiles elements C, N, and O were also determined using the molecules CH, NH, and OH (red triangles in Figs. 2 and 4). There is a very good agreement between the C and O abundances based on high-excitation atomic lines and low-excitation molecular lines, while for N we only present the abundance based on NH. The excellent agreement between atomic and molecular-based differential abundances reinforces the reliability of our adopted atmospheric parameters.

3.1. Abundance versus condensation temperature trend

A possible indication of rocky planet formation (or planet engulfment) can be found in the distribution of the differential elemental abundances as a function of condensation temperature. Refractory elements have high condensation temperature ($T_{\mathrm{C}} \gtrsim 900$ K), easily forming dust, being thus an important component of rocky bodies. Terrestrial planets (or the core of giant planets) may influence the surface abundance of its host star in two ways: first, the accretion of rocky material (planetary engulfment) depleted of hydrogen that enrich the stellar atmosphere in refractories (e.g., Spina et al. 2015; Meléndez et al. 2017; Petrovich & Muñoz 2017); second, the imprisonment of refractory rich material into rocky objects (i.e., planetesimals, rocky planets, and the core of giant planets) that deplete the material accreted by the star during its formation (e.g., Meléndez et al. 2009; Ramírez et al. 2011; Tucci Maia et al. 2014). In the case of planet engulfment, thermohaline mixing should dilute the overabundance in a few million year (Théado & Vauclair 2012), however, the thermohaline mixing could not be as effective and still leave some enhancement on the outer layers of the star that can only be detected with a precision of ~0.01 dex.

An important point to highlight is that the signature of planet formation or planet engulfment is directly connected to the size of the convective zone during the event. If a solar-mass protostar were to go through a fully convective phase that lasted longer than the lifetime of the protoplanetary disk (as it is conventionally accepted; Hayashi 1961), any event of planetary formation

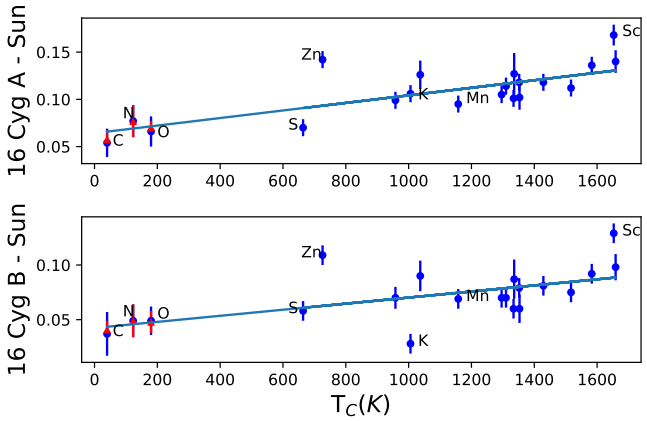

Fig. 2. Elemental abundances of 16 Cyg A (*upper panel*) and B (*lower panel*) based on our manually measured solar abundances as a function of condensation temperature for light elements ($Z \leq 30$). Solid lines represent the linear fits with a slope of $3.99 \pm 0.58 \times 10^{-5}$ for the A component and $2.78 \pm 0.57 \times 10^{-5}$ for 16 Cyg B. Red triangles correspond to the molecule-based abundances of C, N, and O.

that occurs during such a phase would be masked by a significant dilution with the stellar material enclosed into the convective zone, which would homogenize the chemical content throughout the star (see Fig. 2 of Spina et al. 2015).

In contrast to the classic steady accretion, there is the scenario of episodic material accretion onto the star (with observational evidence reported by Liu et al. 2016b). Models that include episodic accretion can reach the stabilization of the convective zone earlier than 10 Myr with initial mass of 10 $M_{\rm Jup}$ and accretion rate bursts of $5 \times 10^{-4}\ M_{\odot}\ {\rm yr}^{-1}$, reaching a final mass of 1 $M_{\odot}$ (Baraffe & Chabrier 2010). Although it is an extreme of their models, it is important to highlight that because of the effects of episodic accretion, the higher the mass of the accretion rate bursts for a given initial mass (or lower the initial mass for a given accretion rate) the greater the impact on the internal structure. Thus, the internal structure reaches the necessary central temperature for the development of the radiative core ($\sim$2–3 $\times 10^6$ K) earlier than what is predicted by the model of a non-accreting star (see Figs. 2 and 4 of Baraffe & Chabrier 2010). This effect makes plausible the assumption that the formation of rocky bodies can chemically alter the surface abundance pattern of its parent star.

Following this premise, Meléndez et al. (2009) suggested that the depletion of refractory elements in the Sun, when compared to a sample of 11 solar twins (without information regarding planets), is due to the formation of terrestrial planets in the solar system (see also further work by Ramírez et al. 2009, 2010). However, in the literature, there are different suggestions for the abundance trend of the Sun with condensation temperature.

Adibekyan et al. (2014) proposed that the trend with condensation temperature is an effect of the chemical evolution of the Galaxy or depends on the birthplace of the star. Investigating the influence of age on solar twins, Nissen (2015) found a strong correlation of α- and s-process elements abundances with stellar age, findings that were confirmed by Tucci Maia et al. (2016) and Spina et al. (2016). According to Önehag et al. (2014), if the star is formed in a dense stellar environment, the gas of the protostellar disk could have its dust cleansed before its birth by radiation of hot stars in the cluster, but recent theoretical estimates by Gustafsson (2018) have suggested that the mechanism is not significant. Gaidos (2015) associated this effect with the gas-dust segregation in the protoplanetary disk. Maldonado & Villaver (2016) found differences in the $T_{\rm c}$ slopes of refractory elements between stars with and without known planets, but this effect depends on the evolutionary stage, since it has been detected on main-sequence and subgiant stars, while no trend is found in their sample of giants. The authors also suggested that there is a correlation of both the mass and age with $T_{\rm c}$.

In this context, the investigation of abundance peculiarities in binary stars with and without planets is essential. This is because in a binary system there is no effect due to the chemical evolution of the Galaxy and other external factors because it would equally affect both stars and thus be minimized in a differential analysis. In this sense, the 16 Cygni system is a very interesting case, in which both components are solar twins with the same age from asteroseismology (van Saders et al. 2016). On top of that, 16 Cyg B has a detected giant planet with a minimal mass of 1.5 Jupiter mass (Cochran et al. 1997) while 16 Cyg A has no planet detected up to now, being thus a key target to study the effect of planets on the chemical composition of stars.

However, the abundance pattern of 16 Cyg A relative to B is still a controversy. A few authors have suggested that there is no difference on the metallicity of the pair (Deliyannis et al. 2000; Schuler et al. 2011; Takeda et al. 2011), while most found abundance differences of about 0.05 dex (Nissen et al. 2017; Adibekyan et al. 2016; Mishenina et al. 2016; Tucci Maia et al. 2014; Ramírez et al. 2011; Laws & Gonzalez 2001; Gonzalez 1998).

3.2. 16 Cygni

A linear fit was performed with orthogonal distance regression (ODS) using the individual abundance errors for each element, excluding K because of its uncertain non-LTE effects. It was necessary to assume a minimum threshold for the abundances uncertainties because some species were returning very small error bars (0.001 dex), thereby heavily impacting the abundance versus condensation temperature slope because some species do not have many lines. In order to address this issue, we adopted a minimum abundance error of 0.009 dex, which is the average error of all species analyzed.

We obtained the slopes $3.99 \pm 0.58 \times 10^{-5}$ and $2.78 \pm 0.57 \times 10^{-5}$ dex K^{-1} for 16 Cyg A − Sun and 16 Cyg B − Sun versus condensation temperature, respectively. In contrast to our past work (Tucci Maia et al. 2014), we did not break the linear fit into two distinct curves for the volatiles and refractory elements, as a simple linear fit represents well the trend with $T_{\rm c}$. We included nitrogen from NH, and for the abundances of C and O we assumed the average between the molecular and atomic abundances.

In Fig. 3 we plot the abundances of the heavy elements ($Z > 30$). In this case, the abundances do not clearly follow the same trend as in the previous case, with slopes $-0.16 \pm 3.99 \times 10^{-5}$ dex K^{-1} and $-0.05 \pm 2.97 \times 10^{-5}$ for 16 Cyg A − Sun and 16 Cyg B − Sun, respectively, with a minimum uncertainty threshold of 0.02 dex in both cases. However, owing to the large errors in the [X/H] and the small range in $T_{\rm c}$ it is not possible to claim if there is indeed a trend by considering only the heavy elements, but we stress that, within the uncertainties, the slope is not actually different from those of $Z \leq 30$. Although no Tc trend is detected, there is a difference Δ(A–B) = 0.043 ± 0.075 dex regarding the abundances of these heavy elements, which somewhat follow the difference of Fe between the stars of the pair, however, owing to the high uncertainty we cannot conclude if this discrepancy is real.

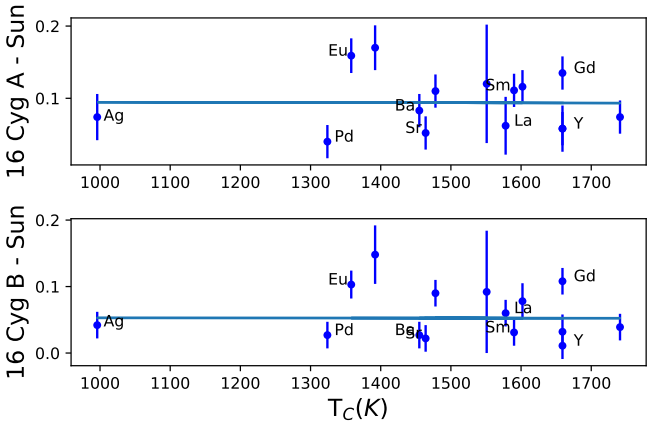

Fig. 3. As Fig. 2 but for the heavy elements ($Z > 30$). There is no clear trend with condensation temperature.

The abundances of 16 Cyg A relative to 16 Cyg B were also determined and are presented in Fig. 4. There is an evident trend between the (A–B) abundances and T_c. The slope of the linear fit (without including the n-capture elements) is $1.56 \pm 0.24 \times 10^{-5}$ dex K^{-1} (with a threshold of 0.005 dex). This result agrees with Tucci Maia et al. (2014; slope $= 1.88 \pm 0.79 \times 10^{-5}$ dex K^{-1}) within error bars, showing once again the consistency and robustness of our analysis. If we include the heavy elements on the fit, we find a slope of $1.38 \pm 0.41 \times 10^{-5}$ (with a threshold of 0.010 dex). Although the abundance of potassium presented in Table 3 has been corrected for non-LTE effects using the grid by Takeda et al. (2002), we did not use it for the linear fit as the non-LTE grid is too sparse for a precise correction. Our slope is also in good agreement with the recent result by Nissen et al. (2017), $+0.98 \pm 0.35 \times 10^{-5}$ dex K^{-1}, based on high-resolution, high-S/N HARPS-N spectra.

3.3. Automated codes

We conducted tests utilizing iSpec[5] version 2016 (Blanco-Cuaresma et al. 2014) and Automatic Routine for line Equivalent widths in stellar Spectra version 2 (ARES; Sousa et al. 2015) to automatically measure the EWs of 16 Cyg A, B, and the Sun to differentially determine the stellar parameters. The aim of these tests is to evaluate if these codes, when applied to high-resolution data and following our methodology (same as in Sect. 2.2), could return a similar result to what we find by "hand". Our motivations for this is to assess if our procedure could be automatized and applied to a bigger sample of stars and still retrieve stellar parameters with the same precision as ours, and to also find out if the chemical composition differences that we found between the 16 Cygni components is consistent by applying different methods of EW meassurement.

As discussed earlier, the differential method minimizes most of the error sources while, for a solar twin sample, the uncertainty is almost entirely related to the EW. One big concern in a differential analysis is the continuum normalization to achieve a consistent continuum placement for all stars being analyzed. In this test, the spectra is the same as our manual analysis, which was previously normalized, and the EW measured following the same line list as ours. In this way, any discrepancy in the values would be due to how each code interprets and places the continuum, and how the fit is performed.

In addition to that, we used another set of spectra with lower resolving power ($R \sim 81\,000$, from Tucci Maia et al. 2014) to evaluate if by using the same tools but providing different resolution spectra, the results could be somewhat discrepant. In Table 4 we present the determined stellar parameters obtained using the EW measurements obtained with the automated codes. Comparing the results, we find that all the codes return stellar parameters in good agreement to ours, based on the "manual" measurements. Overall, as we go to lower resolution, the uncertainty gets higher, as expected, because it can lead to more blends around the lines measured and thus a more contaminated value for the EW. This phenomenon also happens with manual measurements as well, as we can see from the stellar parameters from our previous work (Tucci Maia et al. 2014).

We also used iSpec and ARES to determine the elemental abundance of our sample for the elements with $Z \leq 30$ with the same method and spectra described in the previous section. The trends with condensation temperature are presented in Table 5 with its respective abundance thresholds. In both resolution sets iSpec and ARES returns a T_c slope that is in agreement with our value within error bars. The codes confirm not only that 16 Cyg A is more metal rich than B, but also the existence of T_c trend even though we use spectra with almost half the resolving power (but still high-resolution spectra) as the other. However, iSpec shows a higher significance on its values.

3.4. Li and Be

Lithium and beryllium abundances were determined by performing spectral synthesis calculations, using a method similar to the outlined in Tucci Maia et al. (2015). For lithium, we used the Li-7 doublet at 670.7 nm and, for beryllium, we used the doublet resonance lines of Be II at 313.0420 and 313.1065 nm. The line list for the Li synthesis is from Meléndez et al. (2012), while for Be we used a modified list of Ashwell et al. (2005), as described in Tucci Maia et al. (2015).

For the spectral synthesis, we used the synth driver of the 2014 version of the 1D LTE code MOOG (Sneden 1973). We adopted $A(\mathrm{Be}) = 1.38$ dex as the standard solar Be abundance from Asplund et al. (2009). The model atmospheres were interpolated from the MARCS grid (Gustafsson et al. 2008) using the stellar parameters previously obtained. The abundances of Li were corrected for non-LTE effects using the online grids of the INSPECT project[6]. Beryllium lines are insensitive to non-LTE effects in the solar type stars, according to Asplund (2005).

To determine the macroturbulence line broadening, we first analyzed the line profiles of the Fe I 602.7050, 609.3644, 615.1618, 616.5360, 670.5102 nm, and Ni I 676.7772 lines in the Sun; the synthesis also included a rotational broadening of $v \sin i = 1.9$ km s^{-1} (Bruning 1984) and the instrumental broadening. The macroturbulent velocity found for the Sun is $V_{\mathrm{macro}} = 3.6$ km s^{-1}. For 16 Cygni, we estimate the macroturbulence following the relation of dos Santos et al. (2016), which takes into account the dependence with effective temperature and log g.

With the macroturbulence fixed, $v \sin i$ was estimated for 16 Cyg A and B by fitting the profiles of the six lines mentioned above, also including the instrumental broadening. Table 6 shows the abundances of Li and Be with their estimated macroturbulence and $v \sin i$. In Fig. 5 we show the synthetic spectra of 16 Cyg A and B plotted against the observed spectra.

Comparing our results with previous works in the literature, we found that Li and Be on the binary system 16 Cygni is hardly

[5] iSpec is an open source framework for spectral analysis, see https://www.blancocuaresma.com/s/iSpec

[6] http://inspect-stars.com/

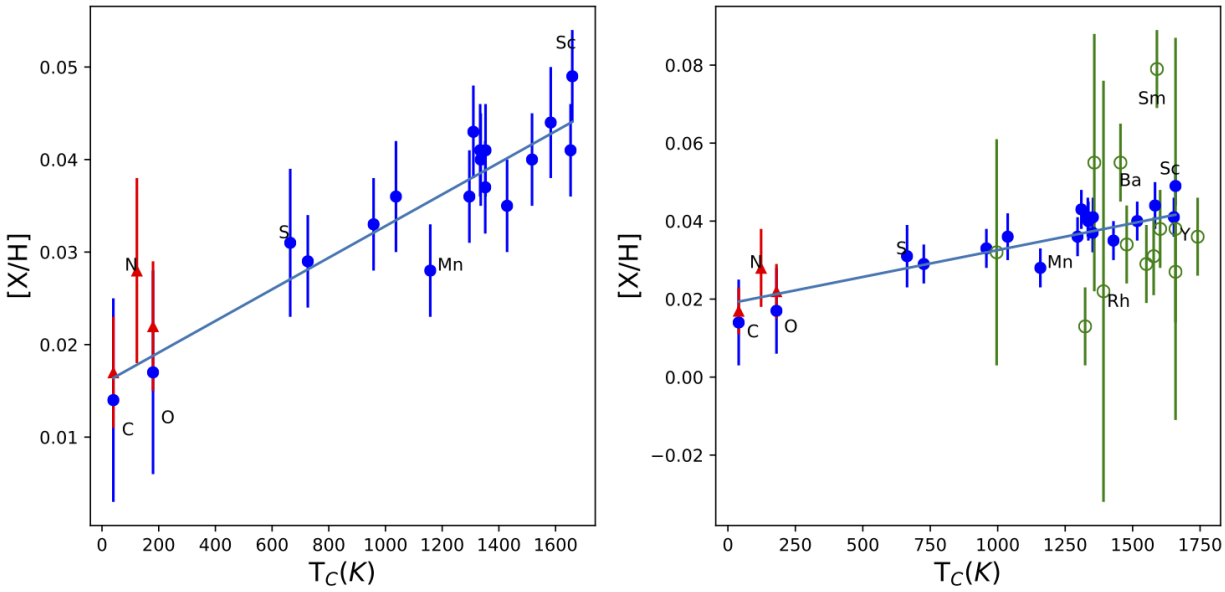

Fig. 4. Differential abundances (manually measured) of (A – B) as a function of T_c for elements with $Z \leq 30$ (*left panel*) also adding the neutron-capture elements (*right panel*). The red triangles correspond to the molecule-based abundances of C, N, and O. The slope found is $1.56 \pm 0.24 \times 10^{-5}$ dex K^{-1} based on the fit to the elements with $Z \leq 30$.

a consensus, but for lithium there is a qualitative agreement in the A component being more abundant in lithium than the B component. It is important to highlight that we found a higher Be abundance on the A component when compared to B, in contrast to the results of Deliyannis et al. (2000) and Garcia Lopez & Perez de Taoro (1998); Takeda et al. (2011), however, did not find any significant Be variation between components, maybe because of the different parameters (including broadening parameters) and different spectra (resolving power, S/N, and normalization).

4. Discussion

Lithium and beryllium are elements that are destroyed at different temperatures (2.5×10^6 and 3.5×10^6 K, respectively) and therefore at different depths in the stellar interiors. According to standard stellar evolution models, these temperatures are only achieved below the base of the convective zone. However, the solar photospheric Li abundance is approximately 150 times lower than the meteoritic value, indicating that extra mixing processes are acting in solar-type stars and need to be taken into account.

In solar-type stars, it is known that Li has a strong correlation with age and surface rotation (Beck et al. 2017; Carlos et al. 2016; Baumann et al. 2010; Do Nascimento et al. 2009), which suggests internal depletion of lithium. However, it is a more challenging task to do the same analysis for Be owing to difficulties related to its detection utilizing instruments from the ground; only two accessible lines of Be II are near the atmospheric cutoff in the UV, at 313 nm, in a heavily populated region of the spectrum. In Tucci Maia et al. (2015), we determined the abundance of Be in a sample of eight solar twins through a "differential" spectral synthesis, where the line list was calibrated to match the observed solar spectrum, which was observed with the same setup as the other stars. We found that the Be content of solar twins is barely depleted, if at all, during the main sequence (~0.04 dex in a time span of 8 Gyrs). Thus, in a probable scenario of a planet being engulfed by its host star, if this event happens after the stabilization of its convective zone, we could expect an enhancement of Li and Be, in a similar way as for refractory elements.

If we analyze our result with this hypothesis in mind, the overabundance of lithium and beryllium on 16 Cyg A relative to B (in addition to the enhancement of refractory elements) could indicate an accretion of mass. In fact, Sandquist et al. (2002) suggested that the Li abundance can be used as a signal of pollution enrichment of the outer layers of solar-type stars, if stellar ages are well known.

The majority of previous studies agree that both components of the binary system have the same stellar ages. However, as seen in Table 7, we found that 16 Cyg A is 0.70 dex more rich in Li than 16 Cyg B, in agreement with the results of Takeda et al. (2011), King et al. (1997), Gonzalez (1998), and Ramírez et al. (2011). Furthermore, on the lithium-age trend of Carlos et al. (2016) and Monroe et al. (2013), 16 Cyg B shows a normal Li abundance for a solar twin of its age, while 16 Cyg A has a Li abundance above the curve; thus, when compared to a sample of solar twins, the A component shows an anomalous abundance of lithium. On top of that, 16 Cyg A also seems to have a higher $v \sin i$ velocity (Table 6), which may indicate momentum transferred by mass accretion.

Gonzalez (1998) also suggested that the odd lithium abundance of 16 Cyg A may be due to planet accretion of a 1–2 Jupiter mass planet. This would increase the abundance not only of Li but of Fe as well. This is reinforced by Mazeh et al. (1997) who propose that the separation between the two stars (semimajor axis of 755 AU; Plávalová & Solovaya 2013) is sufficiently small to permit planet–planet interactions to cause orbit instabilities on the binary pair. Furthermore, the high eccentricity (0.689; Wittenmyer et al. 2007) of 16 Cyg Bb could also be evidence of the interaction between the stars. Similar results were found by Laws & Gonzalez (2001), who found a difference of 0.025 ± 0.009 dex in [Fe/H] between the 16 Cygni pair (the A component being more metal rich), suggesting a self-pollution scenario. Gratton et al. (2001) also investigated abundance differences in six main-sequence binaries with separations on the order of hundreds AU (enough to permit orbit instabilities on possible exoplanets) with components with almost the same mass, using the differential abundance technique (errors on the order of 0.01 dex). Four of these systems do not show any chemical differences between components, while the two remaining

Table 3. Elemental abundances of 16 Cygni system relative to the Sun and to 16 Cyg B.

Z	Species	T_c	$[X/H]_{16\ Cyg\ A}$	Error	$[X/H]_{16\ Cyg\ B}$	Error	$[X/H]_{A-B}$	Error
6	C	40	0.049	0.013	0.033	0.004	0.012	0.009
6	C[(a)]	40	0.058	0.009	0.041	0.008	0.017	0.006
7	N[(a)]	123	0.077	0.017	0.049	0.015	0.028	0.010
8	O	180	0.063	0.014	0.050	0.009	0.012	0.008
8	O[(a)]	180	0.070	0.007	0.048	0.010	0.022	0.007
11	Na	958	0.099	0.008	0.070	0.010	0.033	0.001
12	Mg	1336	0.127	0.022	0.087	0.018	0.040	0.005
13	Al	1653	0.168	0.011	0.129	0.009	0.041	0.004
14	Si	1310	0.114	0.008	0.070	0.007	0.043	0.003
16	S	664	0.070	0.009	0.058	0.009	0.031	0.008
19	K	1006	0.106	0.006	0.028	0.005	0.049	0.001
20	Ca	1517	0.112	0.002	0.075	0.002	0.040	0.003
21	Sc	1659	0.140	0.012	0.098	0.012	0.049	0.004
22	Ti	1583	0.136	0.003	0.092	0.002	0.044	0.006
23	V	1429	0.118	0.006	0.081	0.003	0.035	0.004
24	Cr	1296	0.105	0.004	0.070	0.004	0.036	0.002
25	Mn	1158	0.095	0.005	0.069	0.006	0.028	0.003
26	Fe	1334	0.101	0.004	0.060	0.004	0.041	0.004
27	Co	1352	0.118	0.007	0.079	0.009	0.037	0.003
28	Ni	1353	0.102	0.013	0.060	0.013	0.041	0.004
29	Cu	1037	0.126	0.015	0.090	0.014	0.036	0.006
30	Zn	726	0.142	0.006	0.109	0.005	0.029	0.004
38	Sr	1464	0.052	0.003	0.022	0.002	0.030	0.004
39	Y	1659	0.058	0.008	0.011	0.010	0.041	0.005
40	Zr	1741	0.074	0.017	0.039	0.018	0.036	0.003
44	Ru	1551	0.120	0.082	0.092	0.092	0.029	0.010
45	Rh	1392	0.170	0.031	0.148	0.044	0.022	0.054
46	Pd	1324	0.040	0.007	0.027	0.011	0.013	0.006
47	Ag	996	0.074	0.032	0.042	0.003	0.032	0.029
56	Ba	1455	0.083	0.005	0.027	0.003	0.055	0.001
57	La	1578	0.062	0.040	0.060	0.010	0.031	0.010
58	Ce	1478	0.110	0.020	0.090	0.011	0.034	0.007
60	Nd	1602	0.116	0.021	0.078	0.027	0.038	0.008
62	Sm	1590	0.111	0.009	0.031	0.011	0.079	0.007
63	Eu	1358	0.159	0.024	0.103	0.021	0.055	0.033
64	Gd	1659	0.135	0.016	0.108	0.007	0.027	0.013
66	Dy	1659	0.058	0.032	0.032	0.026	0.038	0.049

Notes. [(a)]Molecular abundance.

Table 4. Atmospheric parameters for 16 Cygni determined with automated EW measurements for $R = 160\,000$ and 81 000 spectra.

	$R = 160\,000$		$R = 81\,000$	
	A	*B*	*A*	*B*
iSpec				
T_{eff} (K)	5834 ± 5	5749 ± 4	5826 ± 15	5753 ± 14
log g (dex)	4.330 ± 0.013	4.360 ± 0.011	4.320 ± 0.042	4.350 ± 0.044
[Fe/H] (dex)	0.103 ± 0.005	0.052 ± 0.003	0.098 ± 0.013	0.057 ± 0.013
vt (km s^{-1})	1.09 ± 0.01	1.02 ± 0.01	1.11 ± 0.03	1.03 ± 0.03
ARES				
T_{eff}	5840 ± 16	5753 ± 15	5813 ± 26	5760 ± 19
log g (dex)	4.330 ± 0.040	4.320 ± 0.038	4.290 ± 0.063	4.390 ± 0.055
[Fe/H] (dex)	0.114 ± 0.013	0.048 ± 0.012	0.091 ± 0.022	0.061 ± 0.017
vt (km s^{-1})	1.07 ± 0.03	1.02 ± 0.03	1.06 ± 0.05	0.97 ± 0.04

Table 5. Slopes of abundances vs. condensation temperature for the elements with $Z \leq 30$ for the EWs measurements from iSpec and ARES for the $R \sim 160\,000$ and 81 000 spectra.

R	iSpec (dex K^{-1})	Min. error (dex)	Significance	ARES (dex K^{-1})	Min. error (dex)	Significance
160 000	$1.11 \pm 0.31 \times 10^{-5}$	0.005	3.58	$0.70 \pm 0.64 \times 10^{-5}$	0.010	1.09
81 000	$1.56 \pm 0.44 \times 10^{-5}$	0.008	3.55	$1.24 \pm 1.04 \times 10^{-5}$	0.019	1.19

Table 6. Abundances of Li and Be for the binary 16 Cyg using spectral synthesis.

	16 Cyg A	16 Cyg B
Li (dex)	1.31 ± 0.03	0.61 ± 0.03
Be (dex)	1.50 ± 0.03	1.43 ± 0.03
$V_{\rm macro}$ (km s^{-1})	3.97 ± 0.25	3.66 ± 0.25
$v \sin i$ (km s^{-1})	1.37 ± 0.04	1.22 ± 0.06

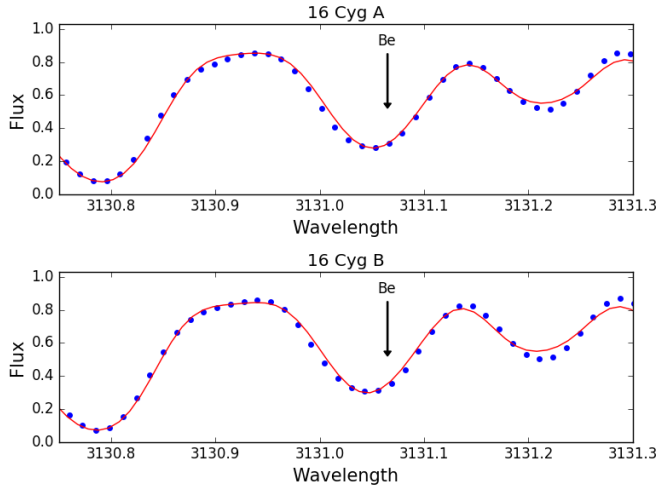

Fig. 5. Comparison between the observed (blue dots) and synthetic (red solid line) spectra of 16 Cyg A (*upper*) and 16 Cyg B (*lower*).

binary systems (HD 219542 and HD 200466) show a clear metallicity difference; the primary stars are more rich in iron (and in the most analyzed elements) than the secondary. The authors also support the idea that the difference in chemical composition of those binary stars is due to infall of rocky material.

By taking into account the hypothesis of planet accretion pollution, we could expect that the Be abundance would also be enriched on the outer layers of the star in a similar way as Li. As discussed earlier, according to Tucci Maia et al. (2015) beryllium is not depleted in a very effective way (if it is at all) on solar twin stars during the main sequence, making it also a good proxy for planet accretion after the stabilization of the convective zone. Comparing the pair of stars, we found that 16 Cyg A has 0.07 ± 0.03 dex more beryllium than 16 Cyg B, in line with the planet engulfment hypothesis.

Following the procedure outlined in Galarza et al. (2016), we estimate that if we add 2.5–3.0 Earth masses of Earth-like material into the convective zone of 16 Cyg B, we would alter the content of Be in about 0.07 dex, thus canceling the abundance difference between the stars. This estimate is close to that derived by Tucci Maia et al. (2014), who derived that the addition of 1.5 Earth mass of a material with a mixture of the composition of the Earth and CM chondrites is necessary to reproduce

Table 7. Comparison of Li and Be abundances.

Star	HD	Li(dex)	Be(dex)
16 Cyg A	186408	1.31 [a]	1.50 [a]
–	–	1.37 [b]	1.34 [b]
–	–	1.27 [c]	0.99 [d]
–	–	1.24 [e]	1.10 [f]
–	–	1.34 [g]	–
16 Cyg B	186427	0.61 [a]	1.43 [a]
–	–	<0.60 [b]	1.37 [b]
–	–	≤0.60 [c]	1.06 [d]
–	–	<0.50 [e]	1.30 [f]
–	–	0.73 [g]	–

References. [a]This work. [b]Takeda et al. (2011). [c]King et al. (1997). [d]Deliyannis et al. (2000). [e]Gonzalez (1998). [f]Garcia Lopez & Perez de Taoro (1998). [g]Ramírez et al. (2011).

the refractory elements abundances as a function of the condensation temperature pattern on 16 Cyg B. However, Tucci Maia et al. (2014) assumed that this abundance pattern is a spectral signature of the 16 Cyg Bb rocky core formation and, now also considering the abundances of Li and Be, it may be a signature of planet accretion rather than planet formation.

In contrast, Théado & Vauclair (2012) discussed that engulfment of rocky planets can induce instabilities on a stellar surface, by the dilution of a metal-rich material in young main-sequence stars, which creates an unstable μ-gradient at the bottom of the convective zone, activating fingering (thermohaline) convection. This would be responsible for the depletion of the abundances that enriched the convective zone, thus quenching any signature of accretion. However, the authors also discussed that the mixing process would not completely erase the enhanced abundances, meaning that the engulfment event would still be detected in the high-precision abundances domain. In this scenario, Deal et al. (2015) argued that during the early periods on the main sequence, 16 Cyg B was able to accrete rocky material from its planetary disk, whereas no accretion may have developed around 16 Cyg A owing to the presence of a red dwarf (16 Cyg C) orbiting at 73 AU around the A component (Turner et al. 2001; Patience et al. 2002). The models of Deal et al. (2015), that take into account the mixing by fingering convection could reproduce the observed difference of lithium on the binary pair by adding 0.66 Earth mass to 16 Cyg B. However, in those same models, Be does not show any depletion with the addition of 0.66 Earth mass with the destruction starting to be more effective with the accretion of higher masses. We note that among the two dozen chemical elements showing abundance differences between 16 Cyg A and B, the model of Deal et al. (2015) can only explain the difference in lithium.

We find this scenario very unlikely because the lithium content of 16 Cyg B seems to be normal for its age when compared

to other solar twins, while 16 Cyg A, on the other hand, displays an enhanced Li content for a solar twin with ~7 Gyr (Carlos et al. 2016; Monroe et al. 2013).

Another explanation for the discrepancy in Li abundances could be different initial rotation rates (Cochran et al. 1997). However, we note that although young solar-type stars of a given mass may have different rotation rates (Lorenzo-Oliveira et al. 2019), they all seem to converge to the same rotation period at an age of about 0.2 Gyr (Barnes 2003), which is much earlier than the age of 16 Cyg. Furthermore, the companion 16 Cyg C at 73 AU may be too far as to have any significant impact on 16 Cyg A.

5. Conclusions

We present a detailed study of elemental abundances on the 16 Cygni solar twin binary system using higher quality data ($R = 160\,000$, $S/N = 1000$ at 670 nm). We confirm the difference of 0.04 dex in [Fe/H] between 16 Cyg A and B. We also confirm the positive trend of differential abundances (A–B) as a function of condensation temperature, in very good agreement with our previous work (Tucci Maia et al. 2014), which was obtained with spectra of lower resolving power and S/N on a different instrument. There is also good agreement with the slope obtained independently by Nissen et al. (2017), and also using a different spectrograph (HARPS-N). We also find the same result by employing the ARES and iSpec codes to measure the EWs. This shows that our differential analysis method is consistent and a powerful tool to unveil physical characteristics that can only be seen with high-precision abundance determinations, and that the T_c trend is a physical phenomenon. Thus, this trend is unlikely to be related to some instrumental effect, as we show that high-quality spectra obtained with different spectrographs (Espadons at CFHT, HDS at Subaru, HARPS-N at the Telescopio Nationale Galileo) give essentially the same results (within error bars).

We also determine the abundance of Li and Be through a "differential" spectral synthesis analysis, using the solar spectrum (obtained with the same instrumental configuration) to calibrate the line list that was used to perform the calculations. We found that 16 Cyg A exhibits an overabundance of not only Li (as reported by previous studies) but of Be as well, relative to 16 Cyg B. This discrepancy is compatible with a 2.5–3.0 Earth masses of earth-like material if we assume a convective zone similar to Sun for both stars. Interestingly, the amount of rocky material needed to explain the Li and Be overabundances is also compatible with the trend of the (A–B) abundances versus condensation temperature, reinforcing thus the hypothesis of planet engulfment, although a similar opposite trend in (B–A) could be attributed to the effect of the rocky core in 16 Cyg B (Tucci Maia et al. 2014). However, the overabundant Li content in 16 Cyg A, above what is expected for its age, suggests that the signature that we are observed is due to a planet engulfment event.

Acknowledgements. M.T.M. acknowledges support by financial support of Joint committee ESO Chile and CNPq (312956/2016-9). J.M., L.S. and D.L.O. thanks FAPESP (2014/15706-9, 2016/20667-8, and 2018/04055-8) and CNPq (Bolsa de produtividade). P.J. acknowledges FONDECYT Iniciación 11170174 grant for financial support.

References

Adibekyan, V. Z., González Hernández, J. I., Delgado Mena, E., et al. 2014, A&A, 564, L15
Adibekyan, V., Delgado-Mena, E., Figueira, P., et al. 2016, A&A, 591, A34
Ashwell, J. F., Jeffries, R. D., Smalley, B., et al. 2005, MNRAS, 363, L81
Asplund, M. 2005, ARA&A, 43, 481
Asplund, M., Grevesse, N., Sauval, A. J., & Scott, P. 2009, ARA&A, 47, 481
Baraffe, I., & Chabrier, G. 2010, A&A, 521, A44
Barnes, S. A. 2003, ApJ, 586, 464
Baumann, P., Ramírez, I., Meléndez, J., Asplund, M., & Lind, K. 2010, A&A, 519, A87
Beck, P. G., do Nascimento, J.-D., Jr., Duarte, T., et al. 2017, A&A, 602, A63
Bellinger, E. P., Basu, S., Hekker, S., & Ball, W. H. 2017, ApJ, 851, 80
Biazzo, K., Gratton, R., Desidera, S., et al. 2015, A&A, 583, A135
Blanco-Cuaresma, S., Soubiran, C., Heiter, U., & Jofré, P. 2014, A&A, 569, A111
Bruning, D. H. 1984, ApJ, 281, 830
Carlos, M., Nissen, P. E., & Meléndez, J. 2016, A&A, 587, A100
Chambers, J. E. 2010, ApJ, 724, 92
Cochran, W., Hatzes, A., Butler, P., & Marcy, G. 1997, ApJ, 483, 457
da Silva, R., Porto de Mello, G. F., Milone, A. C., et al. 2012, A&A, 542, A84
Deal, M., Richard, O., & Vauclair, S. 2015, A&A, 584, A105
Deliyannis, C. P., Cunha, K., King, J. R., & Boesgaard, A. M. 2000, AJ, 119, 2437
Do Nascimento, J. D., Jr., Castro, M., Meléndez, J., et al. 2009, A&A, 501, 687
dos Santos, L. A., Meléndez, J., do Nascimento, J.-D., et al. 2016, A&A, 592, A156
Feltzing, S., Howes, L. M., McMillan, P. J., & Stonkutė, E. 2017, MNRAS, 465, L109
Gaia Collaboration (Brown, A. G. A., et al.) 2018, A&A, 616, A1
Gaidos, E. 2015, ApJ, 804, 40
Galarza, J. Y., Meléndez, J., & Cohen, J. G. 2016, A&A, 589, A65
Garcia Lopez, R. J., & Perez de Taoro, M. R. 1998, A&A, 334, 599
Gonzalez, G. 1998 Brown Dwarfs and Extrasolar Planets, (San Francisco: ASP), 134, 431
Gratton, R. G., Bonanno, G., Claudi, R. U., et al. 2001, A&A, 377, 123
Gustafsson, B. 2018, A&A, 616, A91
Gustafsson, B., Edvardsson, B., Eriksson, K., et al. 2008, A&A, 486, 951
Hayashi, C. 1961, PASJ, 13, 450
Isaacson, H., & Fischer, D. 2010, ApJ, 725, 875
King, J. R., Deliyannis, C. P., Hiltgen, D. D., et al. 1997, AJ, 113, 1871
Laws, C., & Gonzalez, G. 2001, ApJ, 553, 405
Liu, F., Asplund, M., Ramírez, I., Yong, D., & Meléndez, J. 2014, MNRAS, 442, L51
Liu, F., Yong, D., Asplund, M., et al. 2016a, MNRAS, 456, 2636
Liu, H. B., Takami, M., Kudo, T., et al. 2016b, Sci. Adv., 2, e1500875
Liu, F., Yong, D., Asplund, M., et al. 2018, A&A, 614, A138
Lorenzo-Oliveira, D., Porto de Mello, G. F., & Schiavon, R. P. 2016a, A&A, 594, L3
Lorenzo-Oliveira, D., Porto de Mello, G. F., Dutra-Ferreira, L., & Ribas, I. 2016b, A&A, 595, A11
Lorenzo-Oliveira, D., Freitas, F. C., Meléndez, J., et al. 2018, A&A, 619, A73
Lorenzo-Oliveira, D., Meléndez, J., Yana Galarza, J., et al. 2019, MNRAS, 485, L68
Lyra, W., & Porto de Mello, G. F. 2005, A&A, 431, 329
Mack, C. E., III, Schuler, S. C., Stassun, K. G., & Norris, J. 2014, ApJ, 787, 98
Mack, C. E., III, Stassun, K. G., Schuler, S. C., Hebb, L., & Pepper, J. A. 2016, ApJ, 818, 54
Maldonado, J., & Villaver, E. 2016, A&A, 588, A98
Mamajek, E. E., & Hillenbrand, L. A. 2008, ApJ, 687, 1264
Mazeh, T., Krymolowski, Y., & Rosenfeld, G. 1997, ApJ, 477, L103
Meléndez, J., Asplund, M., Gustafsson, B., & Yong, D. 2009, ApJ, 704, L66
Meléndez, J., Bergemann, M., Cohen, J. G., et al. 2012, A&A, 543, A29
Meléndez, J., Bedell, M., Bean, J. L., et al. 2017, A&A, 597, A34
Mermilliod, J.-C., Mermilliod, M., & Hauck, B. 1997, A&AS, 124, 349
Metcalfe, T. S., Creevey, O. L., & Davies, G. R. 2015, ApJ, 811, L37
Mishenina, T., Kovtyukh, V., Soubiran, C., & Adibekyan, V. Z. 2016, MNRAS, 462, 1563
Monroe, T. R., Meléndez, J., Ramírez, I., et al. 2013, ApJ, 774, L32
Montes, D., López-Santiago, J., Fernández-Figueroa, M. J., & Gálvez, M. C. 2001, A&A, 379, 976
Nissen, P. E. 2015, A&A, 579, A52
Nissen, P. E., & Gustafsson, B. 2018, A&ARv, 26, 6
Nissen, P. E., Silva Aguirre, V., Christensen-Dalsgaard, J., et al. 2017, A&A, 608, A112
Noguchi, K., Aoki, W., Kawanomoto, S., et al. 2002, PASJ, 54, 855
Oh, S., Price-Whelan, A. M., Brewer, J. M., et al. 2018, ApJ, 854, 138
Önehag, A., Gustafsson, B., & Korn, A. 2014, A&A, 562, A102
Pasquini, L., & Pallavicini, R. 1991, A&A, 251, 199
Patience, J., White, R. J., Ghez, A. M., et al. 2002, ApJ, 581, 654
Petrovich, C., & Muñoz, D. J. 2017, ApJ, 834, 116
Plávalová, E., & Solovaya, N. A. 2013, AJ, 146, 108

Ramírez, I., Meléndez, J., & Asplund, M. 2009, A&A, 508, L17
Ramírez, I., Asplund, M., Baumann, P., Meléndez, J., & Bensby, T. 2010, A&A, 521, A33
Ramírez, I., Meléndez, J., Cornejo, D., Roederer, I. U., & Fish, J. R. 2011, ApJ, 740, 76
Ramírez, I., Allende Prieto, C., & Lambert, D. L. 2013, ApJ, 764, 78
Ramírez, I., Meléndez, J., Bean, J., et al. 2014, A&A, 572, A48
Ramírez, I., Khanal, S., Aleo, P., et al. 2015, ApJ, 808, 13
Saffe, C., Flores, M., & Buccino, A. 2015, A&A, 582, A17
Saffe, C., Flores, M., Jaque Arancibia, M., Buccino, A., & Jofré, E. 2016, A&A, 588, A81
Saffe, C., Jofré, E., Martioli, E., et al. 2017, A&A, 604, L4
Saffe, C., Jofré, E., Miquelarena, P., et al. 2019, A&A, 625, A39
Sandquist, E. L., Dokter, J. J., Lin, D. N. C., & Mardling, R. A. 2002, ApJ, 572, 1012
Schuler, S. C., Flateau, D., Cunha, K., et al. 2011, ApJ, 732, 55
Sneden, C. A. 1973, PhD Thesis, The University of Texas at Austin, USA
Sousa, S. G. 2014, Determination of Atmospheric Parameters of B-, A-, F- and G-Type Stars, GeoPlanet: Earth and Planetary Sciences, eds., E. Niemczura, B. Smalley, & W. Pych, (Cham: Springer International Publishing), 297
Sousa, S. G., Santos, N. C., Adibekyan, V., Delgado-Mena, E., & Israelian, G. 2015, A&A, 577, A67
Spina, L., Palla, F., Randich, S., et al. 2015, A&A, 582, L6
Spina, L., Meléndez, J., & Ramírez, I. 2016, A&A, 585, A152
Spina, L., Meléndez, J., Karakas, A. I., et al. 2018, MNRAS, 474, 2580
Stetson, P. B., & Pancino, E. 2008, PASP, 120, 1332
Takeda, Y., Zhao, G., Chen, Y.-Q., Qiu, H.-M., & Takada-Hidai, M. 2002, PASJ, 54, 275
Takeda, Y., Tajitsu, A., Honda, S., et al. 2011, PASJ, 63, 697
Théado, S., & Vauclair, S. 2012, ApJ, 744, 123
Teske, J. K., Ghezzi, L., Cunha, K., et al. 2015, ApJ, 801, L10
Teske, J. K., Khanal, S., & Ramírez, I. 2016a, ApJ, 819, 19
Teske, J. K., Shectman, S. A., Vogt, S. S., et al. 2016b, AJ, 152, 167
Tucci Maia, M., Meléndez, J., & Ramírez, I. 2014, ApJ, 790, L2
Tucci Maia, M., Meléndez, J., Castro, M., et al. 2015, A&A, 576, L10
Tucci Maia, M., Ramírez, I., Meléndez, J., et al. 2016, A&A, 590, A32
Turner, N. H., ten Brummelaar, T. A., McAlister, H. A., et al. 2001, AJ, 121, 3254
van Saders, J. L., Ceillier, T., Metcalfe, T. S., et al. 2016, Nature, 529, 181
Wittenmyer, R. A., Endl, M., & Cochran, W. D. 2007, ApJ, 654, 625
Yi, S., Demarque, P., Kim, Y.-C., et al. 2001, ApJS, 136, 417